

Oxygen-mediated suppression of twinning in gas-phase prepared FePt nanoparticles

S. Stappert, B. Rellinghaus^a, M. Acet, and E.F. Wassermann

Exp. Tieftemperaturphysik and SFB 445, Gerhard-Mercator-Universität Duisburg, 47048 Duisburg, Germany

Received 10 September 2002

Published online 3 July 2003 – © EDP Sciences, Società Italiana di Fisica, Springer-Verlag 2003

Abstract. We report on the influence of oxygen on the morphology and crystal structure of gas-phase prepared FePt nanoparticles. The particles are prepared by DC-sputtering in an Ar/He gas mixture. Without any oxygen, the obtained particles are predominantly icosahedra. The additional supply of oxygen leads to significant changes in both the crystal structure and morphology of the FePt nanoparticles. With increasing oxygen concentration, we observe the onset of particle agglomeration and a drop of the particle size. In addition, the crystal structure changes from icosahedral to fcc. These results are ascribed to oxygen mediated changes of the surface properties of the FePt nanoparticles such as the surface diffusivity and the surface free energy.

PACS. 81.07.-b Nanoscale materials and structures: fabrication and characterization – 64.70.Nd Structural transitions in nanoscale materials

1 Introduction

Stoichiometric FePt alloys are promising candidates for magnetic media in future high density magnetic data storage. The thermodynamic equilibrium structure of FePt is a chemically ordered tetragonal phase ($L1_0$), which exhibits a large magnetocrystalline anisotropy and thus allows for the preparation of particularly small and thermally stable magnets. Sun *et al.* [1] have shown that thermal annealing of deposited FePt nanoparticles, which are prepared by a wet chemical routine, causes a phase transformation from the disordered fcc structure to the $L1_0$ structure. However, a disadvantage of this technique is the occurrence of crystal growth and (partial) agglomeration of the particles on the substrate [1, 2]. Recently, we have reported on an alternative gas-phase based method for the preparation of FePt nanoparticles. This method provides the advantage of a possibility to subject the particles to temperatures as high as $T_S = 1273$ K (sintering) in the gas-phase and, thus, prior to their deposition [3, 4]. Typical for the preparation method employed, we obtain predominantly icosahedral, hence, multiply twinned particles (MTP's) [5]. As a consequence, these nanoparticles are superparamagnetic at room temperature and have a relatively low magnetic anisotropy. In order to produce stable magnetic nanoparticles, it is mandatory to avoid the formation of MTP's. It is known that in the gas-phase based preparation of transition metal nanoparticles (*e.g.*, Cu or Ni), the formation of MTP's is suppressed by the additional supply of oxygen, and the formation of single

crystalline and predominantly cuboctahedral particles is preferred [6–8]. We have, therefore, studied the influence of additionally supplied oxygen on the crystallography and morphology of our gas-phase prepared FePt nanoparticles.

2 Experimental

FePt nanoparticles are prepared by DC sputtering from alloy targets in a continuous Ar/He gas flow at pressures of $p = 0.5$ mbar and flow rates of $r_{Ar} = r_{He} = 1.7$ l s⁻¹. The particles are sintered in the gas-phase at $T_S = 873$ K before their deposition onto amorphous carbon films. The experimental details are described elsewhere [3, 5]. To investigate the influence of oxygen on the growth and sintering of the particles, controlled amounts of oxygen are added to the Ar/He gas mixture. The O₂ volume concentration is varied in the range $0.5\% \leq c_{O_2} \leq 6.6\%$. The structure and morphology of the particles are characterized *ex situ* by transmission electron microscopy (TEM).

2.1 Results and discussion

The results of our recent investigations on the gas-phase based preparation of FePt nanoparticles show that the amount of multiply twinned particles (predominantly icosahedra) increases with increasing sintering temperature [3]. In order to study the influence of additionally supplied oxygen on the structure and morphology of the FePt nanoparticles, the present investigation is limited to

^a e-mail: brell1@tphysik.uni-duisburg.de

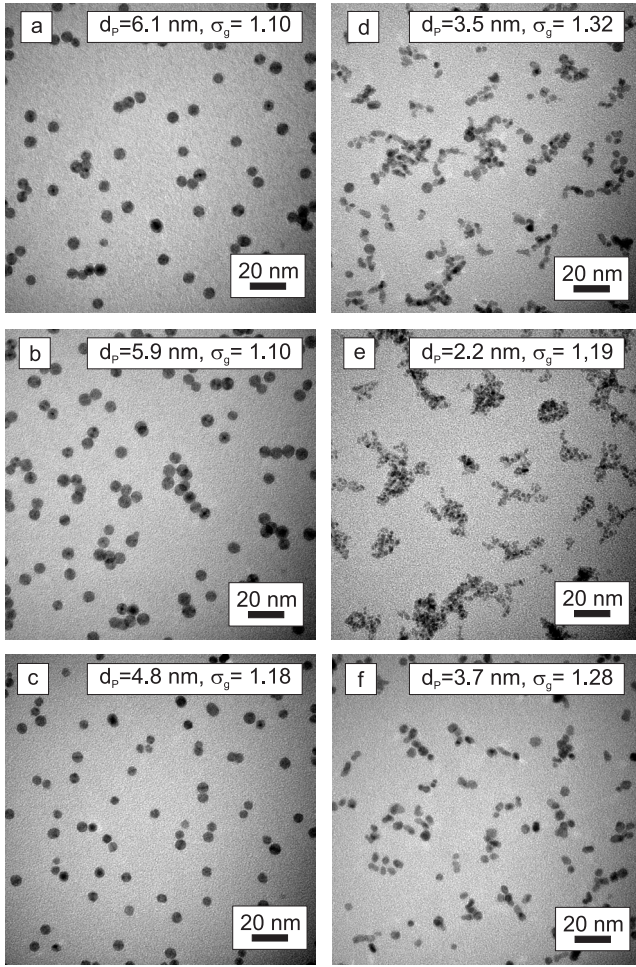


Fig. 1. TEM micrographs of FePt nanoparticles prepared at different oxygen gas flow rates. The corresponding oxygen concentrations are (a) $c_{O_2} = 0$ (no oxygen), (b) $c_{O_2} = 0.5\%$, (c) $c_{O_2} = 0.9\%$, (d) $c_{O_2} = 1.7\%$, (e) $c_{O_2} = 3.4\%$, and (f) $c_{O_2} = 6.6\%$. The particles are sintered in the gas-phase at $T_S = 873$ K.

particles that are sintered at $T_S = 873$ K. At this temperature, the maximum amount of icosahedra is obtained when no oxygen is present.

In Figure 1, we show as an overview six TEM micrographs of FePt nanoparticles which are prepared at various volume concentrations of oxygen. Particles prepared under “clean” conditions, *i.e.* without any additionally supplied oxygen (Fig. 1a), are very monodisperse, non-agglomerated, and exhibit almost spherical morphologies. The mean particle diameter is $d_P = 6.1$ nm, and the geometrical standard deviation is $\sigma_g = 1.1$. This high degree of monodispersity led us to the conclusion that due to the low number concentration, the particles in the nucleation zone grow in a layer-by-layer mode rather than by collision and subsequent coalescence [5].

With increasing volume concentrations of oxygen (*cf.* Figs. 1b–1d), the mean particle size decreases, and the particle size distributions are broadened. At an oxygen concentration of $c_{O_2} = 1.7\%$ (Fig. 1d), we observe the onset

of particle agglomeration. By further increasing the oxygen content to $c_{O_2} = 3.4\%$ (Fig. 1e), we find that the size of the “primary” particles contained within an agglomerate decreases to $1 \text{ nm} \leq d_{\text{prim}} \leq 2 \text{ nm}$. Since sintering at elevated temperatures would always lead to an increase of the particle size and to a compaction of the agglomerates rather than to a downsizing of particles, this dramatic morphological change can only originate from strongly modified growth conditions in the nucleation zone due to the presence of oxygen. Since at the early stage of growth, the particle sizes are smallest, the influence of the particle surface is greatest. There are two important effects of oxygen on free surfaces of (fcc) metals: the presence of oxygen may reduce the surface free energy of metals (*e.g.*, in Cu, γ -Fe, Ni [7,9,11]), and the diffusion of oxygen on a metal surface is slower than the surface self diffusion of the metal. The latter leads to an increased activation energy for surface diffusion (*i.e.* a reduced effective surface diffusivity) in the presence of oxygen (*e.g.*, in Cu, Pt [10,11]). As a consequence of the reduced surface free energy, the size of the critical nucleus for homogeneous nucleation from a supersaturated vapor is decreased, which leads to smaller primary particles in the nucleation zone. Concurrently, the nucleation rate and, thereby, the particle number concentration is increased [12]. Without additionally supplied oxygen, the particle number concentration is just below the critical limit for inter-particle collisions [5]. Apparently, the higher nucleation rate leads to the onset particle-particle collisions and, as a result, agglomeration sets in.

Flagan and Lunden have developed a model where they describe the growth of primarily generated nuclei by collision and coalescence [12]. Here, the growth characteristics are determined by both the probability for inter-particle collisions due to Brownian motion and the velocity of inter-particle coalescence. Hence, the onset of agglomeration is characterized by the equality of the characteristic collision and coalescence times τ_{col} and τ_{coa} , respectively. The coalescence time is mainly determined by the diffusivity and, thus, depends strongly not only on the temperature, but also on the activation energy and the diffusion constant. If we consider surface diffusion the predominant sintering mechanism, the following equations for the coalescence and collision times are obtained [7,12]:

$$\tau_{\text{coa}} \propto d_P^4 T \exp\left(\frac{E_a}{k_B T}\right) \quad (1)$$

$$\tau_{\text{col}} \propto d^{5/2} T^{-1/2}. \quad (2)$$

Here, d_P , T , E_a , and k_B denote the particle diameter, the temperature, the activation energy for diffusion, and the Boltzmann constant, respectively. In Figure 2, we show schematically τ_{coa} (broken lines) and τ_{col} (solid line) as functions of the particle size. The course of τ_{coa} is plotted for two different activation energies. As mentioned above, the presence of oxygen is expected to increase the activation energy for surface diffusion. According to equation (1), this results in an increase of the coalescence time τ_{coa} , whereas the collision time τ_{col} remains almost unaffected (there is only little influence, *e.g.* on the

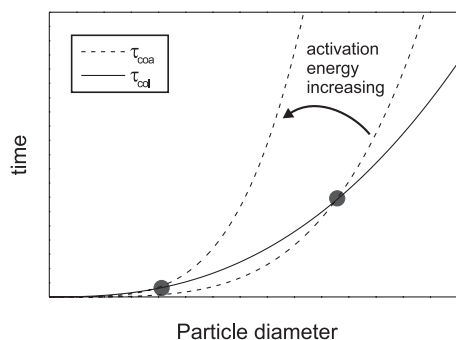


Fig. 2. Schematic plot of the particle size dependence of the characteristic collision time τ_{col} and the coalescence time τ_{coa} .

viscosity of the gas). As a consequence, the onset of agglomeration (*i.e.* the crossing of the broken and solid lines) occurs at smaller particle sizes. Therefore, like the reduction of the surface free energy, the reduced surface diffusivity acts toward the onset of agglomeration at reduced particle sizes.

It is to be expected that such particle agglomerates coalesce at the latest in the sintering oven, which is, however, not observed in our experiments. Apparently, either the residence time in the sintering oven, which is as low as $\tau_S = 0.1$ s, is too short for a significant progress in sintering, or an oxygen layer on the particle surface prevents adjacent primary particles from coalescence.

Surprisingly, a further doubling of the oxygen concentration leads again to individual particles, which are no longer agglomerated (*cf.* Fig. 1f), and the primary particles are even larger than those obtained at lower oxygen concentrations ($d_P = 3.7$ nm, $\sigma_g = 1.28$). We emphasize that this experimental result is reproducible and is in accordance with findings of Olynick *et al.* [7], who report the same behavior for gas-phase prepared Cu nanoparticles. Since the gas pressure is kept constant and, thereby, the collision time is not affected, the coalescence properties in the presence of a critical amount of oxygen are somehow modified. However, this effect lacks any explanation so far.

Besides the oxygen mediated morphological modifications, we also observe changes in the crystal structure of the FePt nanoparticles. In Figure 3, we show a series of representative HRTEM images of particles that are prepared at increasing volume concentrations of oxygen. Particles which are prepared under “clean” conditions (no oxygen) have icosahedral structures [3]. Figure 3a shows as an example a particle that displays the typical HRTEM contrast of an icosahedron along its 2-fold axis [13]. At small oxygen concentrations of $c_{\text{O}_2} = 0.5\%$, there are almost no modifications observable. Still, the predominant structure is icosahedral. The icosahedron presented in Figure 3b is oriented with its 3-fold symmetry axis parallel to the viewing direction. When the oxygen content is further increased, the amount of icosahedra is reduced in favor of single crystal fcc particles, as is exemplified in Figure 3c. In Figure 3d, we show an HRTEM image of agglomerated particles prepared at $c_{\text{O}_2} = 1.7\%$. The crystalline subunits

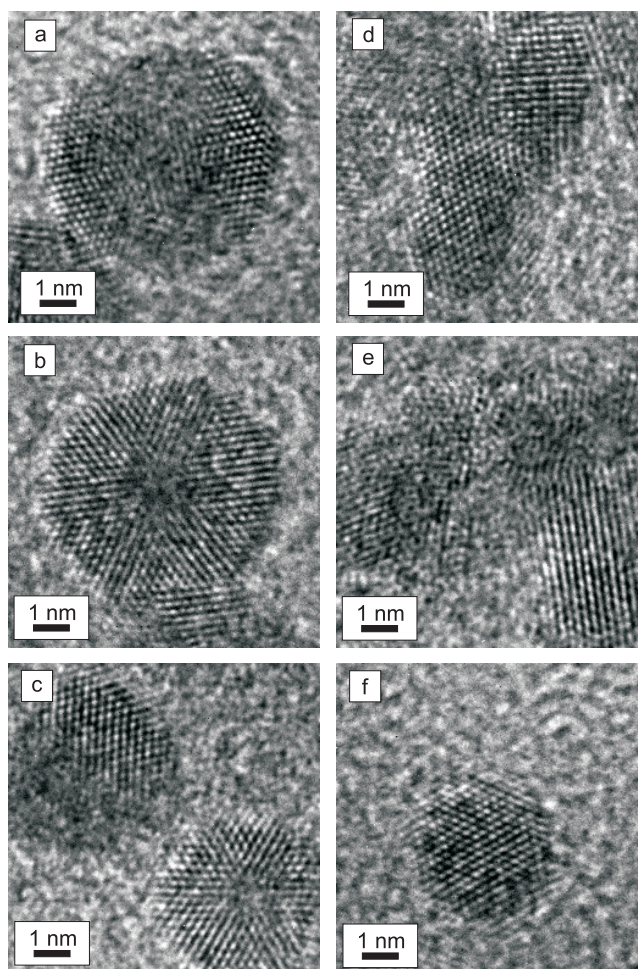


Fig. 3. HRTEM micrographs of particles as prepared at different oxygen concentrations. (a) $c_{\text{O}_2} = 0$ (no oxygen), (b) $c_{\text{O}_2} = 0.5\%$, (c) $c_{\text{O}_2} = 0.9\%$, (d) $c_{\text{O}_2} = 1.7\%$, (e) $c_{\text{O}_2} = 3.4\%$, and (f) $c_{\text{O}_2} = 6.6\%$. The particles are sintered at $T_S = 873$ K.

of the polycrystalline agglomerate are clearly visible. At $c_{\text{O}_2} = 3.4\%$ (Fig. 3e), the degree of crystallinity is further decreased. Concurrent with the unexpected morphological changes due to the modification in the coalescence properties, the crystallite size is significantly increased again at a further increased volume concentration of oxygen of $c_{\text{O}_2} = 6.6\%$. At these oxygen concentrations, we observe mainly single crystal fcc FePt nanoparticles. Figure 3f shows as an example a cuboctahedral particle, which is actually an fcc single crystal with a particular faceting. We like to point that in none of these samples, have we ever found any indication for the occurrence of (crystalline) metal oxides from our HRTEM investigations.

In order to understand the structural changes caused by the additional supply of oxygen, both thermodynamic and kinetic aspects are taken into consideration. As for particle agglomerates, the evolution and stabilization of a certain crystal structure (which is often related to a certain morphology) is significantly influenced by the kinetics of the sintering process. Only in the case of single non-agglomerated particles, which are likely to be

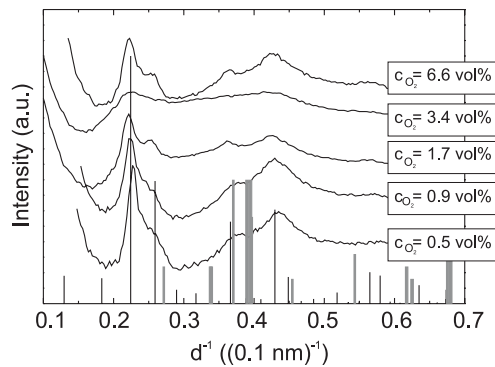


Fig. 4. Electron diffraction pattern of FePt nanoparticles prepared under different oxygen contamination. The black bars indicate the position of Bragg peaks for bulk FePt, the grey bars show peaks of iron oxides.

fully sintered, is it reasonable to assume that they exhibit their thermodynamic equilibrium structure and morphology. FePt nanoparticles, which are prepared under “clean” conditions, do not experience any changes in their structure or morphology when being sintered at temperatures above $T_S \geq 873$ K [3]. It is thus reasonable to assume that these particles are indeed thermally equilibrated. Since decades, it is known that transition metals, which are fcc in the bulk, form multiply twinned particles (MTP’s) such as icosahedra or decahedra in the nanoparticle size regime [14]. At such small particle sizes, the contribution of the surface free energy γ to the total energy becomes important and may even help in shifting the thermodynamic equilibrium, *e.g.*, from (bulk) fcc to icosahedral structures. Thus, the stability of icosahedra which are solely terminated by $\{111\}$ facets, is mainly due to a lower surface free energy γ_{111} of the $\{111\}$ facets as compared to γ_{100} of the $\{100\}$ facets.

In the presence of oxygen, this situation is changed. It is reported in the literature that in case of some transition metals (Cu, γ -Fe), the presence of oxygen leads to a decrease of γ [7,9]. This reduction is found to be more pronounced for $\{100\}$ facets than for $\{111\}$ facets [7]. As a consequence, the $\{100\}$ facets become energetically favored with respect to $\{111\}$ facets leading to a destabilization of icosahedral structures. This argument explains the fact that although the size of the particles is decreasing (which should further stabilize icosahedral structures), we do *not* observe the occurrence of any icosahedra at oxygen concentrations of $c_{O_2} \geq 1.7\%$. We rather observe single crystal fcc FePt nanoparticles.

Electron diffraction observations proves that there are no crystalline metal oxides, in particular iron oxides, present in our samples. In Figure 4, we show a series of electron diffraction patterns (EDP’s) as obtained from the FePt nanoparticles shown in Figures 1 and 3. The position of all observed peaks agree with those of the Bragg peaks for bulk FePt (black bars). With increasing oxygen concentration, the width of the peaks increases indicating a decreasing crystallite size. At $c_{O_2} = 3.4\%$, the EDP is very diffuse, which means that the degree of crystallinity

is very low. In accordance with the results of the HRTEM investigations (Fig. 3f), we observe the recovery of pronounced FePt peaks at $c_{O_2} = 6.6\%$ indicating that the crystallinity improves again. The slight shift of the FePt Bragg peaks towards lower reciprocal lattice spacings with increasing oxygen concentrations indicates an increase of the lattice constant, which may also originate from the reduced surface free energy of the $\{100\}$ facets.

3 Conclusions

FePt nanoparticles are prepared by sputtering in the presence of oxygen. Particles prepared without oxygen are predominantly icosahedra and show no agglomeration. The supply of oxygen leads to the onset of agglomeration which is explained by the enhanced coalescence time due to a reduced surface diffusion in the presence of oxygen. Furthermore, the oxygen causes a destabilization of the icosahedral structure, and the particles acquire a single crystalline fcc structure. This is a consequence of the reduced surface free energy of $\{100\}$ facets as compared to that of $\{111\}$ facets.

References

1. S. Sun, C.B. Murray, D. Weller, L. Folks, A. Moser, *Science* **287**, 1989 (2000)
2. J.W. Harrel, S. Wang, D.E. Nikles, M. Chen, *Appl. Phys. Lett.* **79**, 4393 (2001); H. Zeng, S. Sun, T.S. Vedentam, J.P. Liu, Z.R. Dai, Z.L. Wang, *Appl. Phys. Lett.* **80**, 2583 (2002); Z.R. Dai, S. Sun, Z.L. Wang, *Surf. Sci.* (to appear, 2003)
3. S. Stappert, B. Rellinghaus, M. Acet, E.F. Wassermann, *Mat. Res. Soc. Proc.* **704**, 73 (2002)
4. B. Rellinghaus, S. Stappert, M. Acet, E.F. Wassermann, *Mat. Res. Soc. Proc.* **705**, 315 (2002)
5. S. Stappert, B. Rellinghaus, M. Acet, E.F. Wassermann, *J. Cryst. Growth* (in print, 2003)
6. J. Urban, H. Sack-Kohngel, K. Weiss, *High Temp. Mat. Sci.* **36**, 155 (1996)
7. D.L. Olynick, J.M. Gibson, R.S. Averback, *Phil. Mag. A* **77**, 1205 (1998)
8. S. Stappert, Diploma thesis, Duisburg, 2000
9. L. Li, A. Kida, M. Ohnishi, M. Matsui, *Surf. Sci.* **493**, 120 (2001)
10. M. Yata, H. Rouch, K. Nakamura, *Phys. Rev. B* **56**, 10579 (1997)
11. H. Landolt, R. Börnstein, *Numerical data and functional relationships in science and technology: new series III* (Springer, Berlin, 1992), Vol. 42A, pp. 50-52 and pp. 478-479
12. R.C. Flagan, M.M. Lunden, *Mater. Sci. Eng. A* **204**, 113 (1995)
13. J. Urban, *Cryst. Res. Technol.* **33**, 1009 (1998)
14. J.G. Allpress, J.V. Sanders, *Surf. Sci.* **7**, 1 (1967); S. Ino, S. Ogawa, *J. Phys. Soc. Jpn* **22**, 1365 (1967); L.D. Marks, *Phil. Mag. A* **49**, 81 (1984); C.L. Cleveland, U. Landmann, *J. Chem. Phys.* **94**, 7376 (1991); H. Hofmeister, *Cryst. Res. Technol.* **33**, 3 (1998)
15. C. Hering, *Phys. Rev.* **82**, 87 (1951)